Mining of Mineral Deposits
Volume 17 (2023), Issue 1, 93-100

MMD JOURNAL / MINING.IN.UA

https://doi.org/10.33271/mining17.01.093

Coal from the outburst hazardous mine seams: Spectroscopic study

Serhii Krasnovyd[1*], Andrii Konchits[1], Bella Shanina[1], Mykhailo Valakh[1], Volodymyr Yukhymchuk[1], Mykola Skoryk[2], Oleksandr Molchanov[3], Oleksandr Kamchatny[3]

[1] *V. Lashkaryov Institute of Semiconductor Physics of the National Academy of Sciences of Ukraine, Kyiv, Ukraine*
[2] *G.V. Kurdyumov Institute for Metal Physics of the National Academy of Sciences of Ukraine, Kyiv, Ukraine*
[3] *Branch for Physics of Mining Processes of the M.S. Poliakov Institute of Geotechnical Mechanics of the National Academy of Sciences of Ukraine, Dnipro, Ukraine*

**Corresponding author: e-mail sergkrasnovyd88@gmail.com*

Abstract

Purpose. is to analyze influence mechanisms of physicochemical coal properties on the degree of outburst risk as well as desorption kinetics of methane.

Methods of scanning electron microscopy (SEM), electron paramagnetic resonance (EPR), nuclear magnetic resonance (NMR), infrared spectroscopy (IR) and Raman scattering (RS) have been applied. The samples have been taken from Donbas coal seams varying in their ranks (i.e. carbonization degree).

Findings. It has been identified that in the context of outburst hazardous zones, the ratio between integral intensity of spectral RS bands *D* and *G*, $K = I(D)/I(G)$ shows abnormal dependence upon the nominal amount of volatile compounds connected with the impact by iron impurities. It has been defined that within the ferriferous coal samples, concentration of spins n_s (i.e. the broken carbon bonds) correlates with iron content. Methane adsorption/desorption processes in the studied coal samples have been studied with the help of NMR method; in addition, they have been described using superposition of diffusion and filtration mechanisms.

Originality. It has been understood that high iron content is typical for coal with a greater outburst hazardous degree. The abovementioned iron content and I(D)/I(G) and Ns correlation between the values determines the key role of iron impurities for coal metamorphism processes. For the first time, correlation between the outburst hazardous degree of coal seam and intensity of 3030 cm^{-1} IR band, stipulated by aromatic CH groups where hydrogen is in atomic status, has been identified.

Practical implications. Predictability of outburst risk has been improved in the context of coal seam mining.

Keywords: *ferriferrous coal, methane, coal seam, mine*

1. Introduction

Despite the depletion of natural energy resources of the Earth (i.e. coal, crude oil, and gas), they are still the important component of energy balance of humanity. Among other things, it concerns coal which reserves in some countries (i.e. the USA, China, Australia, Ukraine etc.) are plentiful. In respect of coal deposits, progress is moving towards clean mining and processing technologies, associate methane extraction, and their following efficient use [1]. Moreover, coal deposits are considered from the point of utilization of such gases as CO_2 and mitigation of the global warming risk respectively.

Coal is the natural nanostructured material. Generally, its structure is represented in the form of irregular polymerlike substance where structural elements with different configurations (such as aromatic, aliphatic, and heterocyclic fragments) coexist with carbonic clusters integrated between them [1]-[3]. Coal is a power source, raw material for chemical industry, manufacturing of sorbents, reservoir of different gases (i.e. CH_4, CO_2, and H_2) etc. [4], [5]. Knowledge of local structure of coal, its poriness, magnetic and electric characteristics, and their changes resulting from the external influence is important from the fundamental viewpoint as well as from the practical one [6]-[8]. It is of particular concern that physicochemical characteristics of coal are among the factors of sudden outburst risk in mines [9], [10].

In the process of metamorphism, certain changes in micro- and macrostructure of coal substance take place together with the changes in porous structure as well as in sorption coal properties. The changes are influenced heavily by technogenic processes connected with coal mining. Mineral coal composition and conditions of coal seam formation may result in the development of coal capabilities for different gas-dynamic phenomena (GDP) which manifestation is possible if such seams are extracted [11]-[14]. As a rule, characteristics of outburst hazardous coal differ from 'silent' coal having close V^{daf} values. Usually, V^{daf} is determined as a ratio between volatile matter mass and the total coal mass re-calculated for its dry ashless state. In this work, V^{daf} value varied from 3 up to 46.5%.

Received: 9 November 2022. Accepted: 2 March 2023. Available online: 30 March 2023

Mining of Mineral Deposits. ISSN 2415-3443 (Online) | ISSN 2415-3435 (Print)

Sudden rock or gas (CH_4, CO_2 etc.) outbursts are among the primary reasons of injury cases in coal industry. In addition to high gas content in coal as well as a gradient of changes in gas pressures depending upon the distance from a seam edge [11], intrusions and other abnormal geological conditions [9]-[11], physicochemical coal characteristics [9], [13]-[16] play an essential role in the initiation of outburst gas-dynamic phenomena.

The paper represents research findings of local structure and magnetic resonance features of Donbas coal grades differing in metamorphism degree. Specific attention has been paid to finding correlations between physicochemical coal characteristics and degree of outburst risk in coal seams. The research involved methods of scanning electron microscope (SEM), infrared spectroscopy (IR), electron paramagnetic resonance (EPR) and nuclear magnetic resonance (NMR), Raman scattering (RS). Characteristics of samples from safe and outburst hazardous coal seams have been analyzed and compared.

2. Samples and research methods

Initial samples were taken from different Donbas mines where coal seams differ in rank (i.e. carbonization degree), depth of the mined seams, and their expected outburst risk. The samples were drawn right in a stope after coal was separated from a seam. The standard samples were placed in the sealed containers and delivered to a lab to be analyzed. ~ 4×3×3 mm^3 pieces were cut from the samples to be measured. Table 1 demonstrates composition and characteristics of the studied samples inclusive of SEM/EDX data.

Table 1. General characteristics of coal seams and ultimate composition

Sample	Mine	Seam	Proximate analysis			Ultimate analysis (at. %)				Gas content (m^3/ton)
			V^{daf}, (wt. %)	Ash (%)	Moisture (%)	C	Fe	S	O	
1	Yablunevska	h_{11},	2.0	12.6	4.0	97.17	0.05	1.30	2.16	≤ 5
2	Kirov	h^{up}_{10}	10.2	26.4	1.8	88.10	0.89	3.70	9.67	~ 25
3*	Kholodna balka	h^{up}_{10},	11.3	20.1	2.1	74.45	3.81	3.80	17.55	~ 20
4*	Bazhanov	m_3	24.4	8.2	1.1	87.16	0.34	2.40	10.10	18
5a*	Skochynsky	h'_6	32.0	12.5	1.4	93.17	0.06	0.41	6.14	25
5b*	Skochynsky	h'_6	32.0	12.5	1.3	88.30	0.28	0.46	7.31	25
5c*	Skochynsky	h'_6	32.0	13.0	1.0	47.28	0.84	0.13	36.92	20
6	Pivdenno-Donbaska #1	C_{11}	40.0	5.0	5.3	87.82	0.08	1.20	8.78	< 1
7	Kurakhovska	k_8	46.5	7.3	7.3	90.33	0.10	0.28	9.16	~ 0

* Asterisks mark samples taken from the outburst hazardous seams

Table 1 explains that the samples differ in content of carbon, various impurities (Fe, O, S etc.), V^{daf} values, and gas content. Samples 3, 4, and 5 were drawn from the outburst hazardous seams. Among them, samples 5a, 5b, and 5c were taken while distance R approaching from the sampling point to the outburst hazardous zone centre in Skochynsky mine which happened in 2009. In this regard, 5c sample was drawn from the outburst hazardous zone ($R = 0$). Table 1 shows that a number of the samples differ in relatively high iron content; it especially concerns the samples taken from the outburst hazardous areas. Earlier, paper [10] demonstrated conclusively a role of Fe compounds in coal metamorphism. Moreover, sample 5c has high surface oxygen concentration (~ 37 at. %). It should be mentioned that the research is focused on the comparison between the properties of samples drawn right from the outburst hazardous zone (sample 5c) and adjoining zones (samples 5a and 5b), and other samples, varying in structure, from the seams differing in their outburst hazardous degree.

In the experiments to study kinetics of methane desorption, the samples were saturated with methane. To obtain surface images of the samples and define ultimate composition, SEM Tescan Mira 3 MLU with energy dispersive X-ray spectrometer X-max Oxford Instruments 80 mm^2 SSD X-max detector was applied. RS spectra were excited with the help of Ar-Kr lasering with $\lambda = 457$ mm wave length. They were recorded at room temperature using spectral complex Jobin Ivon T64000. Excitation of spectra as well as recording was performed through a confocal microscope Olympus BX41. To avoid significant heating of the samples in the process of RS spectra measuring, laser power density was selected in such a way to be minimally possible for their reliable recording. While defining frequency location of bands within RS spectrum, an error was not more than 1 cm^{-1}. To exclude impact by random scattering irregularities at the sample surface, RS spectra were measured within several points at the surface of each sample. IR reflectance spectra over 2500-3500 cm^{-1} range were recorded at room temperature using IR Fourier-transform spectrometer Perkin Elmer'Spectrum BXII with ~ 2 cm^{-1} measuring accuracy. Reflectance IR spectra were recorded on the recent cuts.

EPR experiments were carried out with the help of 3 cm spectrometer Radiopan SE/X-2244 with 100 kHz frequency modulation of magnetic field at room temperature. EPR spectra were applied to identify concentration of spins N_s, g-value, and width and shape of EPR lines. Concentration of spins was identified while the signal comparing with a reference sample involving the known spin number. Analysis of the width and shape of EPR lines has helped both importance of ligands for its width and influence by conductance of the samples resulting in asymmetry of the observed EPR line.

Studies of methane desorption kinetics from coal samples were carried out with the help of NMP method. The experimental device, described in paper [17], was applied. The procedure advantage is as follows. It helps obtain information on the methane changes in different phase states of coal in the process of its desorption from sample [1]. Moreover, papers [1], [17] also characterize methods of sample preparation and experimentation. The methane desorption research involved recording of NMR ^1H spectra sequence. A line, corresponding to methane implemented into coal structure, was separated from each spectrum. The line amplitude was proportional to methane quantity in the sample. Desorption characteristics were studied for samples 1, 3, 5a, 5c, and 6 (Table 1) representing all coal grades studied in the research.

3. Results

3.1. Scanning electron microscopy

A surface of the analyzed coal samples have typical morphological features defined by the earlier studies [7]. Figure 1 exemplifies SEM images of sample 5c surface from the outburst hazardous zone (Skochynsky mine) at varying magnification degrees.

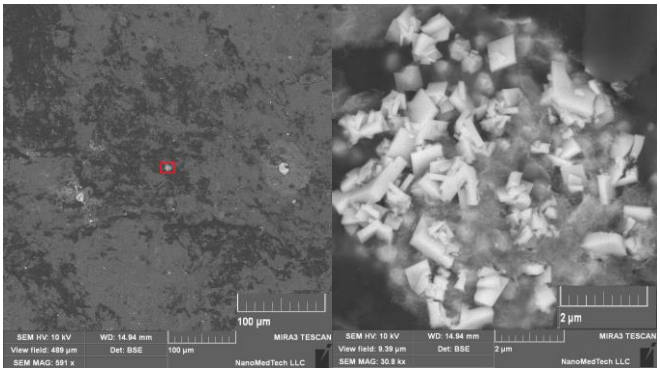

Figure 1. SEM image of sample 5c surface under two magnifications (at the right, you can see central iron-enriched area)

As Figure 1 and Table 1 explain, peculiarity of sample 5c is significant concentration of iron impurity; most likely, it is in the form of pyrite FeS_2.

3.2. RS spectra

Paper [7] informs that RS data have helped identify small carbonic sp^2 clusters in coal which disordering degree grows along with V^{daf} increase. Consequently, the increase of V^{daf} value results in widening of *D* and *G* peaks of RS spectrum. Since *G* peak width depends upon angular disordering of sp^2 aromatic rings, it grows much faster. Also, *K* ratio of integral intensities of *I*(*D*) and *I*(*G*) peaks has been studied; namely, $K = I(D)/I(G)$ according to coal ranks with different V^{daf} values. Paper [5] has identified that *K* value decreases along with V^{daf} value as $K = K_{max} - \alpha(V^{daf})^2$ where the value of numerical parameter $K_{max} = 2.1$ is typical for anthracites. Values of the measured K_{max} and α quantities depend upon numerous factors including frequency of optical excitation.

Figure 2a shows RS spectrum of sample 5c from the outburst hazardous zone; Figure 2b demonstrates $K = I(D)/I(G)$ dependence upon V^{daf} for the samples represented in Table 1. The results confirm partially conclusions by paper [7] on the nature of $K(V^{daf})$ change. At the same time, (V^{daf}) manifests abnormal behaviour for samples 3, 4, and 5c from the outburst hazardous zones for which $K(V^{daf})$ dependence is almost nonavailable. It is indicative that *K* value for 5a, 5b, and 5c from sampling areas, remoted diversely from the outburst hazardous area, increases while approaching the outburst hazardous zone (K_{5a}, $K_{5b} < K_{5c}$) (Fig. 2b). Except for sample 5c, the observed data are described by a following Function (1) being similar to that one defined in paper [7]; however, in this case $K_{max} = 1.23$:

$$I(D)/I(G) = 1.23 - 0.00017\left(V^{daf}\right)^2. \quad (1)$$

Sample 5c, taken from the outburst hazardous zone, demonstrates abnormally high $K = 1.19$ value being typical for anthracites (Fig. 2b). At the same time, nominal V^{daf} values for h'_6 seam coal in Skochynsky mine and for anthracites vary greatly (Table 1).

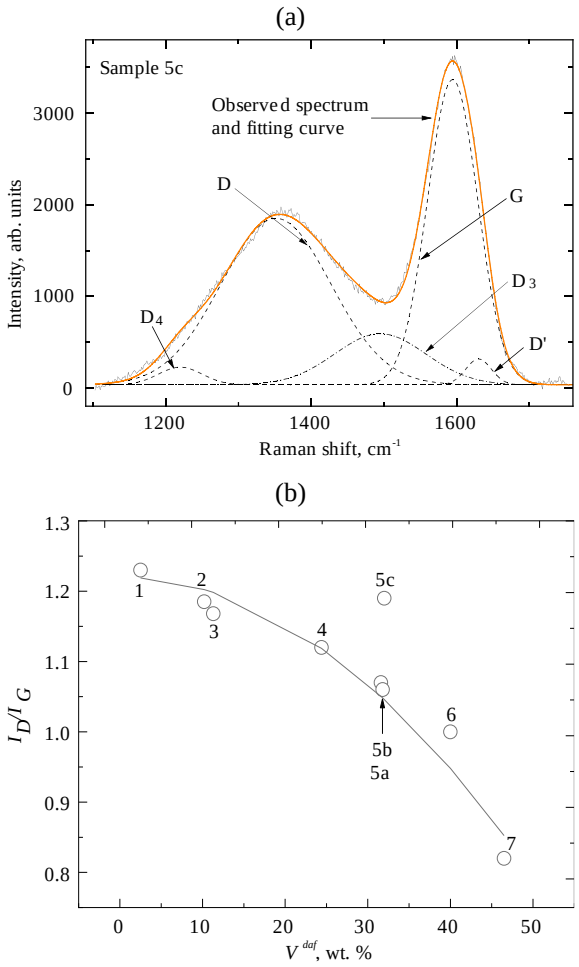

Figure 2. Raman spectra study: (a) representative Raman spectrum of sample 5c taken from the outburst hazardous zone; (b) I_D/I_G change depending upon V^{daf}

Figure 2 shows a solid line calculated according to Formula (1); $\lambda_{exc} = 457$ nm. Actually, sample 5c is heavily carbonated young anthracite formed probably because of thermal metamorphism induced by magmatic intrusion [12], [13]. As a result, we observe $K = I(D)/I(G)$ value for sample 5c coinciding with sample 1 of pure anthracite. Samples 5a and 5b from the areas, distant from the outburst hazardous zone, are a mixture of heavily carbonized clusters and disordered aromatic sp^2 rings decreasing eventually the *K* value. Along with the approaching outburst hazardous place, availability of *K* gradient denotes presence of pressure gradient and, consequently, increase in the outburst likelihood [11].

3.3. IR spectroscopy

Figure 3 demonstrates spectra of infrared reflection of coal samples drawn from the potentially safe and outburst hazardous seams in Donbas mines.

Spectra in Figure 3 show clearly four bands. Bands within 2856 and 2920 cm^{-1} belong to symmetrical and asymmetrical tensile C-H braces in methylene (CH_2) of aliphatic groups; and a band within 3030 cm^{-1} is attributed to CH links of aromatic groups [18]-[21].

Figure 3 explains that samples of outburst hazardous formations are characterized by the availability of intensive 3030 cm^{-1} band connected with oscillations of extensions in aromatic structures.

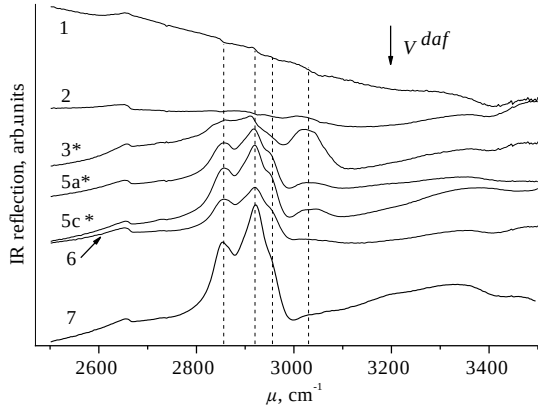

Figure 3. Infrared reflection spectra of coal samples taken from the safe and outburst seams of different mines (Asterisk marks samples taken from outburst coal seams)

3.4. Electron paramagnetic resonance

3.4.1. Paramagnetic characteristics of coal samples from safe zones

The broken bonds of carbon atoms (BBC) are the key carriers of paramagnetic properties of coal [1]-[3], [6], [7]. A number of papers consider BBC from more general viewpoint as one of the basic energy suppliers in katagenesis of organic substance in rocks [22]. The paper regards paramagnetic coal properties in the context of influence by a structure and availability of magmatic intrusions in coal seams on their outburst risk.

Figure 4 shows dependence of concentration of paramagnetic centres (PCs) (BBC) in coal samples, drawn from safe seams, with different V^{daf} values. In the context of the samples, concentration of spins N_s decreases along with V^{daf} increase according to the law:

$$N_s = \frac{10^{18}\, spin \cdot gm^{-1} \cdot 27.14}{\left(1 + 0.286 \cdot V^{daf}\right)}. \qquad (2)$$

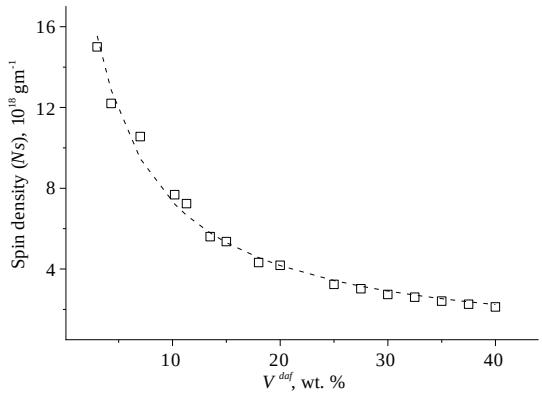

Figure 4. Spin concentration in coal samples, having different V^{daf} values, taken from safe coal seams in Donbas mines; iron concentration within the samples is minor; the dotted curve has been calculated on Formula (2)

Many characteristics of such coal ranks (including role of radicals in association with coal under hydropyrolysis) were studied earlier [7]-[9], [23]. Generally, Function (2), describing behaviour of spin density, is in keeping with the data. Porosity, i.e. availability of open and closed pores, is an important feature of highly metamorphized coal. Consequently, width of EPR lines of coal samples depends upon proper widening mechanisms (i.e. dipole orientational, superhyperfine, exchangeable etc.) as well as upon PC interaction with paramagnetic molecular oxygen penetrating into pores [7], [9]. Figures 5 and 6 demonstrate some features of interaction with oxygen in terms of sample 1 (anthracite, Yablunevska mine) (Table 1).

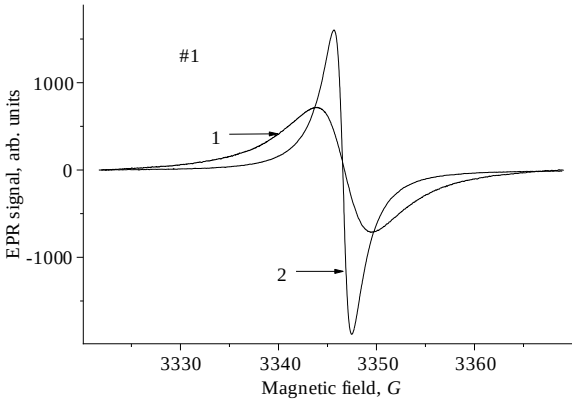

Figure 5. EPR spectrum of a sample 1 in the air (curve 1) and after pumping under T = 300 K (curve 2)

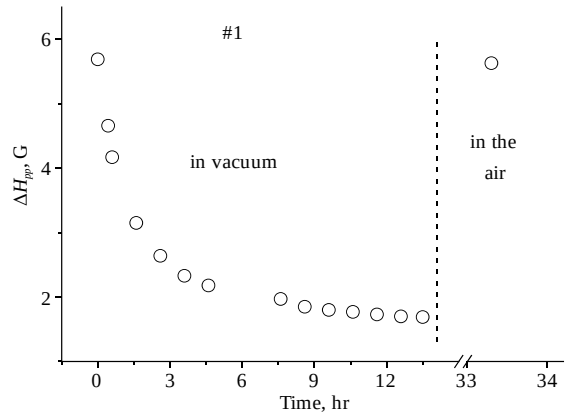

Figure 6. Dependence of EPR line width of sample 1 upon gradual oxygen desorption under the conditions of continuous pumping if T = 300 K

EPR spectrum of sample 1 (Fig. 5) consists of a single line with g factor $g = 2.0029$ being typical for BBC [7]. ΔH_{pp} EPR line width in the air is stipulated by the availability of molecular oxygen in the sample pores since the line experiences more than three-time narrowing after oxygen desorption (5.7 G down to 1.7 G) (Figs. 5 and 6). Slow process of oxygen adsorption/desorption at room temperature is the characteristic feature of coal samples from the mine (Fig. 6). The abovementioned denotes large number of the closed pores, within which oxygen crosses a natural surface barrier while desorbing.

After vacuum annealing at $T = 550$°C, characteristics of sample 1 vary significantly (Fig. 7). EPR spectrum of the annealed and pumped out sample 1 (Fig. 7) is asymmetric line of Dyson shape denoting significant conductivity of the sample. The spectrum has been described using EPR theory for conductive samples [24], [25].

Figure 7 shows the result for $d >> \delta$, δ_e conditions where d is sample thickness; δ is skin layer thickness determined with the help of the sample conductivity and UHF field; and δ_e is diffusion length of electrons for the period of spin relaxation T_2. In terms of dimensionless units, EPR line shape is identified by means of the only parameter being $R^2 = T_D / T_2 = (\delta / \delta_e)^2$. In this regard, the true resonance magnetic field H_{res} is out of phase with a situation where amplitude of signal derivative is equal to zero since within the conductive samples a signal is the combination of absorption and dispersion signals.

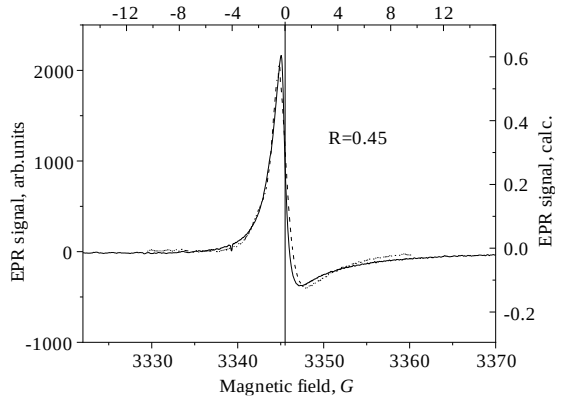

Figure 7. EPR spectrum of sample 1 after half-hour vacuum annealing at T = 550ºC; the dotted lines are theoretical description (the spectrum has been recorded under the sample pumping conditions at room temperature, ν = 9380 MHz)

Resulting from alignment, the experimental spectrum has been described using the parameters: g = 2.0032; R = 0.45; and ΔH = 1.3 G. It should be mentioned that such a line shape was observed earlier for naturally pyrolyzed anthracite samples [7].

If sample-air contact takes place then EPR line width within the annealed sample 1 increases up to ΔH_{pp} = 11 G value. It is almost twice more than the line width before anneal denoting the increased concentration of the absorbed oxygen owing to the heightened porosity of the sample.

3.4.2. Paramagnetic characteristics of samples taken from outburst hazardous seams

To compare structural and EPR properties of samples, drawn from safe and outburst hazardous coal seams, the paragraph considers paramagnetic characteristics of samples from the outburst hazardous mines. Table 1, representing results of SEM/EDX analysis, explains that high iron concentration is in samples 3, 4, and 5c correlating with a high outburst hazardous degree of the seams, from which the samples were drawn. Moreover, sample 3 shows higher sulfur concentration; and surface oxygen concentration of sample 5c, taken from the outburst zone, is abnormally high. Probably, it is a result of outburst. High Fe concentration within the samples is confirmed independently by EPR data. Actually, after the samples from Table 1 were annealed in the air for 30 minutes at 500ºC temperature, strong magnetic resonance signals with g = 2.13 and $\Delta H_{pp} \approx$ 1.4 kG, belonging to iron oxides, were demonstrated only by samples 3 (Fig. 8), 4, and 5c.

Figure 9 demonstrates EPR spectra of samples 5a and 5c taken from the outburst outlying zone and from the outburst zone respectively. Comparison of Figure 9a, b explains that importance of a narrow line 2 for the spectrum intensity increases after outburst. Hence, the number of areas, available for oxygen pumping (i.e. open pores and surface), grows, i.e. coal microstructure after the outburst becomes more porous.

Turn to the importance of iron. To understand iron impact on GDP, it is required to observe correlation between concentration of paramagnetic centres (i.e. the broken carbon bonds) in coal samples and their iron content. Figure 10 represents the obtained data.

Figure 10 demonstrates clearly the correlation between concentration of paramagnetic defects and iron content of the analyzed samples. Sample 3 has shown maximum concentration of defects with the highest iron content (i.e. 3.81 at. %) among the analyzed series of samples.

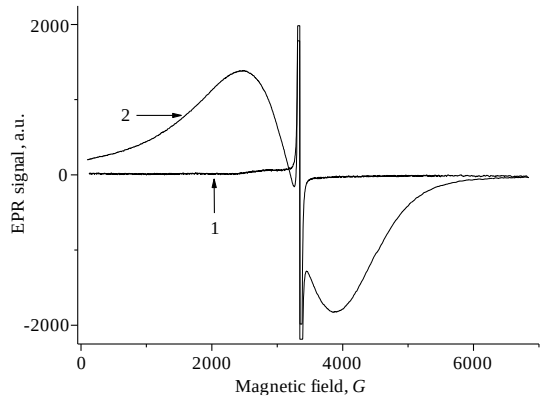

Figure 8. EPR spectra of the initial sample 3 (curve 1) and after its 30-minute anneal at T = 500ºC (curve 2); narrow line in the centre belongs to the broken carbon bonds (g = 2.0029)

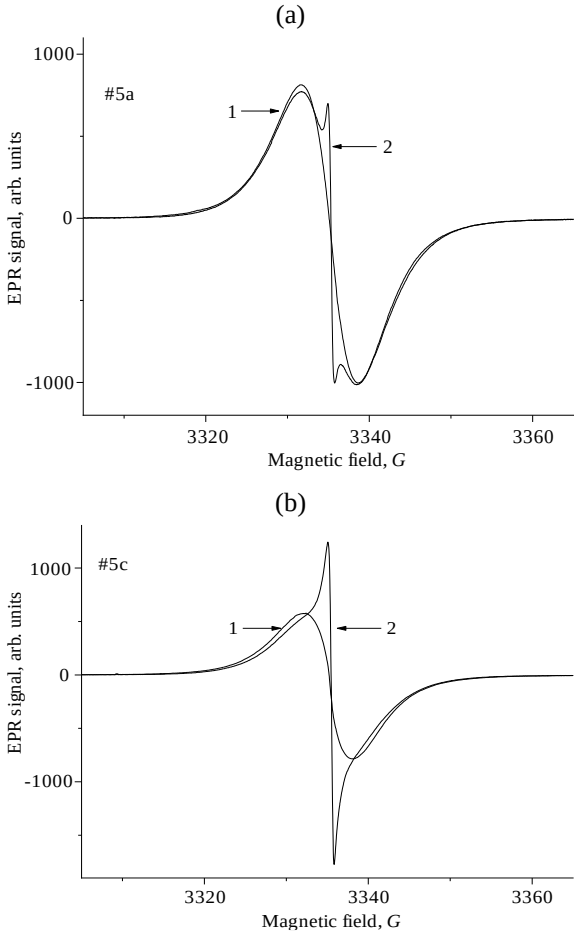

Figure 9. EPR spectra of samples 5a and 5c taken from the outburst outlying zone (a) and from outburst zone (b); 1 – in the air samples; 2 – samples after 1-hour pumping at T = 130ºC, and ν = 9350 MHz

3.5. Nuclear magnetic resonance

Kinetics of methane desorption has been studied using samples 1, 3, 5a, 5c, 6 from the coal grades varying in their metamorphism (Table 1). All the samples are methane saturated. Figure 11 shows relative over time change in A amplitude of NMR ^{1}H line corresponding to methane amount in the samples as well as kinetics of methane release from them.

It is known [1], [26] that kinetics of methane desorption from fossil coal can be described using superposition of two mechanisms being diffusional and filtrational.

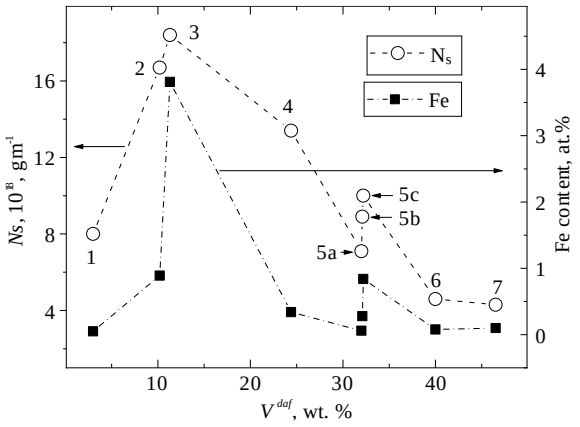

Figure 10. Concentration of paramagnetic centres N_s and iron content of coal samples from Table 1; the samples are numerated similarly to Table 1 and Figure 2b; the dotted lines are guide for eyes

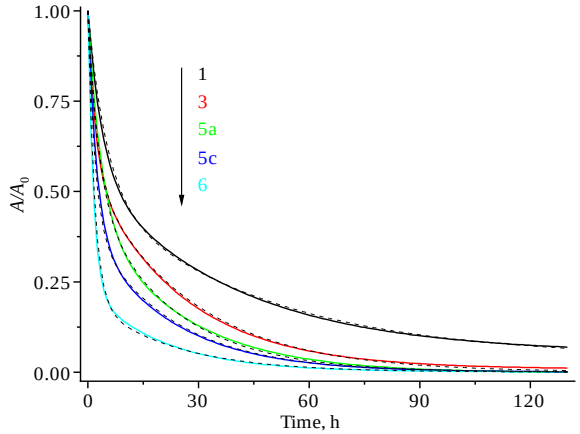

Figure 11. Relative over time change in A amplitude of NMR ^1H line of the occluded methane from the entire NMR spectrum of the analyzed coal samples; solid lines are experimental; the dotted lines are analytical calculated on Formula (3) with the coefficients from Table 2

Filtration is a complex process involving absorption to the closed pore surface, dissociation of molecules into atoms, and diffusion through a pore wall. Gas, contained in the closed pores and dissolved in coal substance, penetrates into partially free open pores and cracks the crossing potential barriers to get to the surface through diffusion. Curves of methane desorption from coal, shown in Figure 11, are described sufficiently by the total of two downward exponents:

$$A(t) = a \cdot \exp\left(\frac{-t}{t_1}\right) + b \cdot \exp\left(\frac{-t}{t_2}\right) + k_0, \qquad (3)$$

where:

$A(t)$ – amplitude of NMR line;

t_1 and t_2 – typical for two mechanisms;

a and b – relative contributions of two mechanisms;

k_0 – residual methane if $t -> \infty$, $a + b + k_0 = A(t = 0) = A_0$.

Typical times of methane desorption from coal depend upon a metamorphism degree connected with the microstructure of coal substance characteristics, availability of cracks, and porous coal structure. Table 2 represents the obtained values of typical desorption times for the analyzed samples.

Samples of coal grade *D* (6), and anthracite (1) absorb more methane per unit weight than coal grades *K* (5a, 5c), *T* (3) being of average metamorphism degree.

Table 2. Characteristics of methane desorption from coal samples*

Sample	1 (*A*)	3 (*T*)	5a (*K*)	5c (*K*)	6 (*D*)
t_1 (filtration), h	45.45	27.00	21.74	22.20	22.20
t_2 (diffusion), h	5.00	2.22	2.86	1.92	1.82
a	0.50	0.45	0.50	0.60	0.80
b	0.46	0.55	0.50	0.40	0.20
k_0	0.04	0.00	0.00	0.00	0.00

*Asterisks mark coal grades: *A* is anthracite; *T* is semianthracite; *K* is coking coal; and *D* is long-flaming coal

However, if methane (and oxygen, Figure 6) release from the compact fine anthracite structure for a long time, desorption from open coarse-porous takes the shortest period for coal grade *D*. Coal grades, characterized by average metamorphism degree, demonstrate longer desorption time to compare with *D* coal grade. It should be mentioned that in the context of coal grade *K* (5c) sample, taken from the outburst hazardous area of h′$_6$ seam in O.O. Skochynsky mine, period of desorption process (and its components) is shorter than in the context of 5a coal sample drawn from a quiet zone of the same seam. Outburst results in partial destruction of macroscopic coal structure as well as its microstructure reducing the time of diffusion component of methane desorption process.

4. Discussion

Explanation of RS spectra behaviour, observed in Figure 2b, may lie in consideration of specific characteristics of coal within the outburst hazardous zones [12]-[14]. According to [13], [14] models, intrusion areas of rocks, erupted because of tectonic processes, are particularly outburst hazardous. The latter results in the accelerated, so-called thermal coal metamorphism. Consequently, the coal is modified up to anthracite within the intrusion area. It is quite possible that coal from the outburst in O.O. Skochynsky mine exemplifies such accelerated metamorphism processes. At the same time, the main share of the mined seam is unaffected by the intrusion. It is reasonably believed that abnormal geological conditions combined with the accumulated gas amount influence heavily the outburst risk [12].

Comparison of the broken carbon bond concentration upon V^{daf} (Figs. 4 and 10) for the samples from safe and outburst hazardous zones respectively shows critical distinction between them. A law of inverse N_s – V^{daf} ratio is typical for the samples from safe seams since it is connected with volatile-matter yield from the closed pores as well as with the release of atomic hydrogen closing the broken bonds. Iron is the main factor for the samples taken from the outburst hazardous seams since it favours the accelerated methanogenesis within the open pores. Correlation between the iron content and outburst risk of coal seams means that iron is a component in the process of gas dynamic phenomena formation as papers [10], [11], [14] predicted. Another fundamental fact, impacting the outburst hazard, takes place. A number of papers denote that under outburst, methane amount may excess significantly the average gas content of a seam [12], [27]. It has been assumed that the circumstance can depend upon the formation of extra methane amount during outburst because of atomic hydrogen attachment to CH_3 molecule [23]. Certainly, the abovementioned needs considerable concentration of atomic hydrogen. Results on IR reflection, shown in Figure 3, confirm openly the fact. Indeed, Figure 3 demonstrates clear correlation between the identified outburst risk of coal seams and intensity of 3030 cm^{-1} band, attributed to CH aromatic groups [16]-[18].

The experiment with samples, saturated with methane, and kinetics of its desorption has shown that release velocity from the closed pores is an order of magnitude less than from the open ones in the context of each sample regardless of a metamorphism degree. Desorption processes accelerate in coal samples, drawn from the outburst zone, owing to changes in microstructure which supports additionally by EPR data (Fig. 9).

5. Conclusions

The samples, taken from the "silent" and outburst hazardous coal seams in Donbas mines, have been studied. Comparative analysis of their properties explains that the outburst hazardous zones are characterized by high iron content. The samples, drawn right from the outburst zone (after outburst) also have high surface oxygen content.

RS spectra of coal samples from the outburst hazardous areas demonstrate high $I(D)/I(G)$ ratio being typical for anthracite regardless of nominal V^{daf} value. Such behaviour is in keeping with a model of intrusive acceleration of metamorphism processes as well as with the fact that such zones are of high outburst risk.

Ferruginous coal shows correlation between iron content and concentration of paramagnetic defects being the broken bonds of carbon (BBC). The abovementioned means that iron impurity is a catalyzer of methane formation in coal as well as a factor of increase in BBC concentration. A structure of the samples, taken right from the outburst zone, becomes more porous; the fact is supported by EPR BBC line widening in the air at the expense of their interaction with molecular oxygen adsorbed within the pores. Pyrolysis of coal samples with the average and high metamorphism degree has similar effect.

The samples from the outburst hazardous coal seams are characterized by intensive 3030 cm^{-1} IR band stipulated by aromatic CH groups, within which hydrogen is in its atomic state. During outburst, it favours formation of excessive methane owing to hydrogen atom attachment to CH_3 molecule (IR 2956 cm^{-1} band); as a result, increase in destructive outburst force happens.

According to the obtained NMR data, methane adsorption/desorption processes within the analyzed coal samples are described with the help of superposition of two (i.e. diffusional and filtrational) mechanisms. In the context of samples, taken right from the outburst area, a period of diffusional component of desorption experiences 1.5 times decrease at the expense of partial destruction of coal macro- and microstructure.

Acknowledgements

Authors from ISP appreciate the support by the National Academy of Sciences of Ukraine (Project #23/21-H). The authors express gratitude to I.B. Yanchuk for the help in experiments on IR spectroscopy.

References

[1] Alexeev, A.D. (2010). *Physics of coal and mining processes*. Kyiv, Ukraine: Naukova Dumka.

[2] Krzesinska, M., Pilawa, B., & Pusz, S. (2006). The physical parameters of different rank coals related to their degree of cross-linking and the caking ability. *Energy Fuels*, *20*(3), 1103-1110. https://doi.org/10.1021/ef050284e

[3] Mathews, J.P., & Chaffee, A.L. (2012). The molecular representations of coal – A review. *Fuel*, *96*(1), 1-14. https://doi.org/10.1016/j.fuel.2011.11.025

[4] Jaleh, B., Nasrollahzadeh, M., Eslamipanah, M., Nasri, A., Shabanlou, E., Manwar, N., Zboril, R., Fornasiero, P., & Gawande, M.B. (2022). The role of carbon-based materials for fuel cells performance. *Carbon*, (198), 301-352. https://doi.org/10.1016/j.carbon.2022.07.023

[5] Kwak, C.H., Lim, C., Kim, S., & Lee, Y.-S. (2022) Surface modification of carbon materials and its application as adsorbents. *Journal of Industrial and Engineering Chemistry*, (116), 21-31. https://doi.org/10.1016/j.jiec.2022.08.043

[6] Mrozowski, S. (1988). ESR studies of carbonization and coalification processes Part II. Biological materials. *Carbon*, *26*(4), 531-541. https://doi.org/10.1016/0008-6223(88)90152-2

[7] Konchits, A.A., Shanina, B.D., Valakh, M.Ya., Yanchuk, I.B., Yukhymchuk, V.O., Alexeev, A.D., Vasilenko, T.A., Molchanov, A.N., & Kirillov, A.K. (2012). Local structure, paramagnetic properties, and porosity of natural coals: Spectroscopic studies. *Journal of Applied Physics*, (112), 043504. https://doi.org/10.1063/1.4745015

[8] Niu, B., Niu, M., Zhang, J., Liu, R., Zhong, H., & Hu, H. (2022). Novel insight into the mechanism of coal hydropyrolysis using deuterium tracer method. *Fuel*, (321), 124109. https://doi.org/10.1016/j.fuel.2022.124109

[9] Grinberg, O.Y., Williams, B.B., Runge A.E., Grinberg, S.A., Wilcox, D.F., Swartz, H.M., & Freed, J.H. (2007). Oxygen effects on the EPR signals from wood charcoals: Experimental results and the development of a model. *Journal of Physical Chemistry B*, *111*(46), 13316-13324. https://doi.org/10.1021/jp072656l

[10] Ulyanova, E.V., Molchanov, A.N., Prokhorov, I.Y., & Grinyov, V.G. (2014). Fine structure of Raman spectra in coals of different ranks. *International Journal of Coal Geology*, *121*(1), 37-43. https://doi.org/10.1016/j.coal.2013.10.014

[11] Skoblik, A.P., Shanina, B.D., Kolesnik, V.N., Konchits, A.A., & Gavriljuk, V.G. (2012). A modeling for the effect of iron compounds on methane formation in coal. *Fuel*, (98), 124-130. https://doi.org/10.1016/j.fuel.2012.01.080

[12] Black, D.J. (2019). Review of coal and gas outburst in Australian underground coal mines. *International Journal of Mining Science and Technology*, *29*(6), 815-824. https://doi.org/10.1016/j.ijmst.2019.01.007

[13] Dai, Sh., & Ren, D. (2007). Effects of magmatic intrusion on mineralogy and geochemistry of coals from the Fengfeng-Handan coalfield, Hebei, China. *Energy & Fuels*, *21*(3), 1663-1673. https://doi.org/10.1021/ef060618f

[14] Nikolin, V.I., Zabolotnyj, A.G., & Lunev, S.G. (1999). *Modern concepts of the nature of the outburst hazard and the emission mechanism as a scientific basis for occupational safety*. Donetsk, Ukraine.

[15] Lama, R.D., & Bodziony, J. (1998). Management of outbursts in underground coal mines. *International Journal of Coal Geology*, *35*(1-4), 83-115. https://doi.org/10.1016/S0166-5162(97)00037-2

[16] Skoblik, A.P., Shanina, B.D., Okulov, S.M., Ulyanova, E.V., Shpak, A.P., & Gavriljuk, V.G. (2011). Effect of iron compounds on hyperfine interactions and methane formation in the coal. *Journal of Applied Physics*, (110), 013706. https://doi.org/10.1063/1.3601741

[17] Molchanov, A.N. (2011). An improved set of equipment for studying the sorption properties of fossil coals. *Physical and Technical Problems of Mining*, (14), 42-53.

[18] Konchits, A.A., Shanina, B.D., Krasnovyd, S.V., Yukhymchuk, V.O., Hreshchuk, O.M., Valakh, M.Ya., Skoryk, M.A., Kulinich, S.A., Belyaev, A.E., & Iarmolenko, D.A. (2018). Structure and electronic properties of biomorphic carbon matrices and SiC ceramics prepared on their basis. *Journal of Applied Physics*, (124), 135703. https://doi.org/10.1063/1.5042844

[19] E.L. Fuller, JR., & Smyrl, N.R. (1990). Chemistry and structure of coals: Hydrogen bonding structures evaluated by diffuse reflectance infrared spectroscopy. *Applied Spectroscopy*, *44*(3), 451-461. https://doi.org/10.1366/0003702904086056

[20] Machnikowska, H., Krzton, A., & Machnikowski, J. (2002). The characterization of coal macerals by diffuse reflectance infrared spectroscopy. *Fuel*, *81*(2), 245-252. https://doi.org/10.1016/S0016-2361(01)00125-9

[21] Yao, S., Zhang, K., Jiao, K., & Hu, W. (2011). Evolution of coal structures: FTIR analyses of experimental simulations and naturally matured coals in the Ordos Basin, China. *Energy Exploration & Exploitation*, *29*(1), 1-19. https://doi.org/10.1260/0144-5987.29.1.1

[22] Brechuntsov, A.M., & Nesterov, I.I. (2011). Oil of bituminous argillaceous, siliceous-argillaceous, and carbonate-siliceous-argillaceous rocks. *Gornye Vedomosti*, *6*(85), 30-61.

[23] Frolkov, G.D., & Frolkov, A.G. (2011). Correlation between the sudden and regular releases of coal-bed methane and the structures of the organic matter of natural coals. *Solid Fuel Chemistry*, *45*(1), 7-11. https://doi.org/10.3103/S0361521911010046

[24] Poole, Jr. (1997). *Electron spin resonance: A comprehensive treatise on experimental techniques*. Mineola, United States: Dover Publications 921 p.

[25] Gavriljuk, V.G., Efimenko, S.P., Smouk, Ye.E., Smouk, S.Yu., Shanina, B.D., Baran, N.P., & Maksimenko, V.M. (1993). Electron-spin-resonance study of electron properties in nitrogen and carbon austenites. *Physical Review B*, *48*(5), 3224-3229. https://doi.org/10.1103/PhysRevB.48.3224

[26] Liu, Z., Lin, X., Wang, Z., Zhang, Z., Chen, R., Wang, L., & Li., W. (2022). Modeling and experimental study on methane diffusivity in coal mass under in-situ high stress conditions: A better understanding of gas extraction. *Fuel*, (321), 124078. https://doi.org/10.1016/j.fuel.2022.124078

[27] Shpak, A.P., Alexeev, A.D., Ulyanova, E.V., Trachevsky, V.V., & Chistokletov, V.N. (2012). Nature of methane generation in coal beds. *Reports of the National Academy of Sciences of Ukraine*, (6), 105-110.

Вугілля з викидонебезпечних пластів шахт: спектроскопічне дослідження

С. Красновид, А. Кончиць, Б. Шаніна, М. Валах, В. Юхимчук, М. Скорик, О. Молчанов, О. Камчатний

Мета. Дослідити механізми впливу фізико-хімічних властивостей вугілля на ступінь викидної небезпеки та кінетику десорбції метану.

Методика. Використано методи скануючої електронної мікроскопії (СЕМ), електронного парамагнітного резонансу (ЕПР), ядерного магнітного резонансу (ЯМР), інфрачервоної спектроскопії (ІЧ) та комбінаційного розсіювання світла (КРС). Зразки відібрано з вугільних пластів різного рангу (ступеню карбонізації) з шахт Донецького басейну.

Результати. Встановлено, що для зразків з викидонебезпечних зон відношення інтегральних інтенсивностей спектральних смуг КРС *D* і *G*, $K = I(D)/I(G)$ показує аномальну залежність від номінального обсягу летких речовин V^{daf}, яка пов'язана з впливом домішок заліза. Виявлено, що у залізовмісних зразках вугілля концентрація спінів Ns (обірвані зв'язки вуглецю) корелює із вмістом заліза. Процеси адсорбції/десорбції метану у вивчених зразках вугілля досліджено методом ЯМР та описано суперпозицією двох механізмів – дифузійного та фільтраційного.

Наукова новизна. Визначено, що для вугілля із шахтних пластів з високим ступенем викидонебезпечності характерно підвищений вміст заліза. Вищезазначена кореляція між вмістом заліза та величинами $I(D)/I(G)$ і Ns встановлює важливу роль домішок заліза у процесах метаморфізма вугілля. Вперше виявлено кореляцію між ступенем викидонебезпечності вугільних пластів та інтенсивністю ІЧ-смуги 3030 $см^{-1}$, обумовленої ароматичними СН-групами, в яких водень знаходиться в атомарному стані.

Практична значимість. Покращення прогнозованості небезпеки викидів при розробці вугільних пластів

Ключові слова: *залізовмісне вугілля, метан, вугільний пласт, шахта*